The Structure of Dark Matter Halos in an Annihilating Dark Matter Model

Matthew W. Craig *

Department of Physics and Astronomy, Minnesota State University Moorhead, Moorhead, MN 56563

Marc Davis

Astronomy and Physics Departments, University of California, Berkeley CA 94720

Abstract

The inability of standard non-interacting cold dark matter (CDM) to account for the small scale structure of individual galaxies has led to the suggestion that the dark matter may undergo elastic and/or inelastic scattering. We simulate the evolution of an isolated dark matter halo which undergoes both scattering and annihilation. Annihilations produce a core that grows with time due to adiabatic expansion of the core as the relativistic annihilation products flow out of the core, lessening the binding energy. An effective annihilation cross section per unit mass equal to .03 $\mathrm{cm}^2\ \mathrm{g}^{-1}$ (100 $\mathrm{km\ s}^{-1}/v$) with a scattering cross section per unit mass of .6 $\mathrm{cm\ g}^{-1}$ produces a 3 kpc core in a 10^{10} $\mathrm{M}_\odot$ halo that persists for 100 dynamical times. The same cross section leads to a core of only 120 pc in a rich cluster. In addition to creating to cores, annihilation should erase structure on scales below $\sim 3 \times 10^8$ $\mathrm{M}_\odot$. Annihilating dark matter provides a mechanism for solving some of the problems of non-interacting CDM, at the expense of introducing a contrived particle physics model.

Key words: dark matter, methods: N-body simulations, galaxies: dwarf
PACS: 95.35, 95.75.P, 98.52.W

* Corresponding author.
Email addresses: mcraig@mnstate.edu (Matthew W. Craig), marc@astro.berkeley.edu (Marc Davis).

1 Introduction

Discrepancies between the Cold Dark Matter (CDM) model and observations on galactic scales (Salucci, 2001; Moore, 1994; Flores & Primack, 1994; Burkert, 1995; Salucci & Burkert, 2000; Moore, 2001; Sellwood & Kosowsky, 2000; Weiner et al., 2001b) have led to recent revival of the suggestion that the dark matter is self-interacting (Spergel & Steinhardt, 2000).

Simulations of halo formation in a CDM universe predict that dark matter halos have a cuspy inner profile. Most simulations find that, at small radii, $\rho \propto r^{\alpha}$, with $\alpha \approx -1$ to -1.5 (Navarro et al., 1996b; Ghigna et al., 2000; Jing & Suto, 2000; Klypin et al., 2000). An inner density profile this steep may be consistent with the dark matter density profile inferred from many high surface brightness galaxies and clusters of galaxies (Eke et al. (2000), but see Borriello & Salucci (2001)). However, low surface brightness galaxies, and dwarf irregular galaxies in particular, require an inner density profile which is less steep (Moore (1994); Burkert (1995); Flores & Primack (1994); for a contradictory view see van den Bosch & Swaters (2000)). In addition, Debattista & Sellwood (2000) have emphasized that too much dark matter in the centers of galaxies is incompatible with rotating bars, which are common in massive galaxies such as the Milky Way.

A separate problem for standard CDM model is that it predicts many more dark matter satellites of a Milky Way-sized galaxy than are observed (Moore et al., 1999; Klypin et al., 1999). This substructure cannot simply be dark satellites in which stars have not formed, because they would thicken the disk of the Milky Way as they passed through the plane of the disk.

While it is possible that the inclusion of baryonic physics would lead to a less cuspy dark matter halo, perhaps due to supernova driven gas outflow in dwarf galaxies (Navarro et al., 1996a), this seems unlikely, as cooling baryons would lead to further concentration of the dark matter halo through adiabatic compression. Exploding gaseous disks will drive a strong wind off the plane, but most simulations show that the cold, dense component of a multi-phase medium would be difficult to remove (Mac Low, 2001). Furthermore, these solutions to the cusp problem does not address the problem of too much substructure on small scales.

Recent attention has focused instead on the possibility that the dark matter is self-interacting. A remarkable number of different models have been proposed. For example, several authors have considered a model in which the dark matter is a self-interacting scalar field with quartic potential (Peebles, 2000; Peebles & Vilenkin, 1999; Goodman, 2000; Riotto & Tkachev, 2000). Hu et al. (2000) have suggested a model in which cores are produced in dwarf galaxies due to

the wave nature of dark matter, if the matter is an ultra-light scalar particle. Another interacting dark matter candidate is Q-balls, non-topological solitons with properties that allow it to scatter, possibly with a time-dependent cross-section, or to merge (Kusenko & Steinhardt, 2001). Several authors have simulated halo evolution and formation in scenarios in which the dark matter scatters. All authors agree that on short time scales, scattering reduces the logarithmic slope of the inner density profile substantially; some authors have found that the inner density profile subsequently steepens as the halo undergoes core collapse (Kochanek & White, 2000; Yoshida et al., 2000), while others disagree (Burkert, 2000; Davé et al., 2001).

Self-annihilating dark matter is another possible solution to the problem (Kaplinghat et al., 2000), although the particle physics must be carefully contrived so that the dark matter does not completely self-annihilate in the early universe. An analytic calculation of the density of a self-annihilating dark matter halo demonstrates the formation of a core. Physically, the core develops because annihilation becomes very efficient at removing mass from the halo above a density that depends on the annihilation cross section. Kaplinghat et al. (2000) point out that this annihilation also causes an adiabatic expansion of the halo, and numerically calculate the effects of adiabatic expansion; the core density including expansion is smaller than that predicted from annihilation alone by a factor of ten (for dwarf galaxies) to three (for clusters). In addition, Hui (2001) points out that unitarity bounds require that annihilation be accompanied by scattering.

In this paper, we simulate the behavior of an isolated dark matter halo which undergoes both scattering and annihilation. In section 2, we describe our dark matter model and our simulation methods. In section 3 we present the results of our simulations, and in section 4 we compare our results with those of previous authors.

2 Model

2.1 Initial halo and units

We simulated the evolution of an isolated halo; the initial density profile is the Hernquist (1990) profile,

$$\rho = \frac{M}{2\pi r(r + r_s)^3}, \tag{1}$$

where M is the total mass of the halo, and r_s is the scale radius. We take the dynamical time for this model to be the circular orbit time at the scale radius r_s,

$$t_{dyn} = 4\pi\sqrt{\frac{r_s^3}{GM}} \tag{2}$$

In the simulations below, we work in units in which $G = 1$, $M = 1$, and $r_s = 1$.

The profile has been generated to guarantee that the center of mass of the halo is also the origin used in calculating the density of the Hernquist profile. We first choose the energy for each particle, then select a radius for the particle; these determine the magnitude of the velocity of the particle. We adopt an isotropic velocity distribution. For each particle generated with position $\mathbf{r}$, a second particle is generated with position $-\mathbf{r}$; the second particle has the same energy as the first. The distribution is truncated at a radius of $100r_s$. The direction of the velocity of each particle is generated independently, but the net velocity of the halo is set to zero.

2.2 Model for scattering and annihilation.

We adopt a model similar to that used by Burkert (2000). The probability for interaction for a particle which moves a distance Δx in time step Δt is

$$P = \frac{\Delta x}{\lambda}, \tag{3}$$

where $\lambda = 1/(n\sigma)$ is the mean free path for interactions; this expression is valid only when $\Delta x \ll \lambda$. Our simulations include both scattering and annihilation. We use the notation σ_a^* to denote the annihilation cross section per unit mass and σ_s^* to denote the scattering cross section per unit mass.

The probability that a *pair* of particles scatters in time step Δt is

$$P_{s,ij} = \sigma_s^* v_{ij} \rho_l \Delta t, \tag{4}$$

where ρ_l is the local density, and v_{ij} is the *relative* velocity of particles i and j. Scattering is completely elastic, and is isotropic in the center of momentum frame of the pair of particles.

As pointed out by Kaplinghat et al. (2000), only s-wave annihilation is consistent with observations. For s-wave annihilation, $\sigma|v|$ is independent of velocity,

so that the cross section for annihilation per unit mass, σ_a^*, is given by

$$\sigma_a^* = \frac{\tilde{\sigma}_a}{m}\frac{v_a}{v}, \tag{5}$$

where $\tilde{\sigma}_a v_a$ is determined by the scattering potential. The numerical value we assume for the scattering cross section is given below.

The probability for an annihilation interaction in time step Δt is:

$$P_a = \sigma_a^* \rho_l v \Delta t = \frac{\tilde{\sigma}_a v_a}{m}\rho_l \Delta t, \tag{6}$$

where ρ_l is the local density. The annihilation probability is independent of velocity.

We model the decay of the dark matter particles represented by our simulation particles by assigning to each simulation particle a probability for annihilation given by equation (6). If the local density is large enough, P_a is the probability that some of the dark matter particles represented by the simulation particle would interact and decay. If a simulation particle decays, its mass m_i is reduced by fraction F,

$$m_{i,new} = (1 - F)m_{i,old}. \tag{7}$$

Thus, the effective probability for annihilation of individual dark matter particles in our model is the product FP_a. The mass lost in an annihilation is a pre-set fraction of the current mass of the particle undergoing annihilation. In other words, the *fractional* mass lost in an annihilation is held fixed. The absolute mass loss, $m_{i,old} - m_{i,new}$, decreases as a particle undergoing repeated annihilation loses mass.

2.3 Numerical Parameters

Our simulations were run on a GRAPE3-AF special purpose hardware card (Okumura et al., 1993) using a direct summation code. The time step was chosen to be small enough to satisfy both the Courant condition and to ensure that $v\Delta t < \lambda$. Each run contained 30,000 particles. Detailed numerical parameters for each run are shown in Table 1. Runs S0A0, S3A0, and S3A1 ran for roughly 10 dynamical times with approximately 2100 steps per dynamical time; a fourth run, S.3A.1, was done with a much larger Plummer softening and time step; it ran for 100 dynamical times with approximately 400 steps per dynamical time.

Table 1
Simulation Parameters

Name	σ_s^*	$\sigma_a^* v$	ϵ	Δt	N_{steps}	t_f/t_{dyn}
S0A0	0	0	0.01	0.006	20,000	9.55
S3A0	3.0	0	0.01	0.006	15,750	7.52
S3A1	3.0	1.5	0.01	0.006	20,000	9.55
S.3A.1	0.3	0.15	0.05	0.03	40000	95.5

One run, S0A0, had no interactions, and was used to determine the stability of the integration. The run S3A0 had no annihilations, but non-zero scattering cross-section. Two runs with annihilation and scattering were performed. One, S3A1, was short (the final time was a tenth of a Hubble time assuming a $10^{10}\mathrm{M}_\odot$ halo), but had the same scattering cross-section as the scattering-only run. The other, S.3A.1, ran for ten times longer, with both annihilation and scattering cross section reduced by a factor of ten. In both annihilation runs the scattering and annihilation *probabilities* are equal at the scale radius; inside of that radius scattering will be enhanced relative to annihilation because the scattering probability increases with velocity. The fractional mass loss per annihilation in both was $F = 5\%$.

The cross section per unit mass for scattering can be calculated in physical units from

$$\sigma^*_{phys,s} = .48\sigma^*_s \left(\frac{10^{10}M_\odot}{M}\right)\left(\frac{R_s}{1\mathrm{kpc}}\right)^2 \ \mathrm{cm}^2\mathrm{g}^{-1}. \tag{8}$$

The cross-section for annihilation is given by

$$\sigma^*_{phys,a} = .98\sigma^*_a \left(\frac{10^{10}M_\odot}{M}\right)\left(\frac{R_s}{1\mathrm{kpc}}\right)^2\left(\frac{100\mathrm{kms}^{-1}}{v}\right) \ \mathrm{cm}^2\mathrm{g}^{-1} \tag{9}$$

For $R_s = 2$ kpc and $M = 10^{10}\mathrm{M}_\odot$, the half mass dynamical time is .168 Gyr. Our cross-sections are $\sigma_s^* = 5.76\mathrm{cm}^2\mathrm{g}^{-1}$ and $\sigma_a^* = 5.88\mathrm{cm}^2\mathrm{g}^{-1}(100\mathrm{kms}^{-1}/v)$ for the run S3A1; in the run S.3A.1, both cross sections are a factor of ten smaller. Our values of σ_s^* span the range suggested by Wandelt et al. (2000). Kochanek & White (2000) considered a broader range of values for σ_s^*; our choice for our runs with the largest scattering cross section is in the middle of their range.

In both annihilating runs, we chose our annihilation cross section to be comparable to the scattering cross section. However, this annihilation cross section in the run S3A1 is about 300 times larger than that suggested by Kaplinghat et al. (2000) based on fits of rotation curves to dwarf galaxies. The run

S.3A.1, with an annihilation cross section ten times smaller, is closer to what they suggest. With a mass loss factor F of 5%, the effective cross section $F\sigma_a^*$ is comparable to the value required to match observations. In both cases, the scattering cross section is above the minimum required by unitarity bounds (Hui, 2001).

3 Results

The inclusion of annihilation in our simulations causes a reduction in the central density of the halo. Figure 1 shows the evolution in the density profile of a halo with both annihilation and scattering; the top panel shows a short run with high cross section (S3A1), and the bottom a run with smaller cross section run for longer time (S.3A.1). The central density rapidly decreases, and remains low for the duration of the simulations, about 100 (10) dynamical times for run S.3A.1 (S3A1).

The core is not due to numerical effects. The force softening is .05 (.01) in the run S.3A.1 (S3A1); the flattening of the inner density profile we observe occurs at radii 2–10 (10–50) times larger than that and is unlikely to have been caused by softening. To test the stability of our code and the effects of our relatively limited particle number, we ran a simulation with no interactions for ten dynamical times. The simulation with no interactions S0A0 shows no evidence of the development of a core. The density profile of the halo was essentially unchanged over the course of the simulation. Figure 1 shows the beginning profile and the final profile for this run.

We have examined the mechanism by which the core forms in our interaction simulations. There are three related mechanisms one might imagine contributing to the development of a core. First, mass lost due to annihilation and the disappearance of the relativistic decay products from the halo directly decreases the central density of the halo. Second, this direct mass loss reduces the gravitational potential of the halo, causing particles in the central region to become less bound. Third, energy is transferred from the central region of the halo outward by scattering, depressing the central density.

Although scattering at first suppresses the central density, core collapse begins fairly rapidly in halos with scattering only, as reported by Kochanek & White (2000). We have run one simulation with scattering alone to determine whether the core that initially forms persists. The results of this run are shown in Figure 2. The central density initially drops and then increases after a few dynamical times. [1] In the absence of annihilation, scattering does not produce

[1] This run was terminated after 5.8 dynamical times. At that point, the central

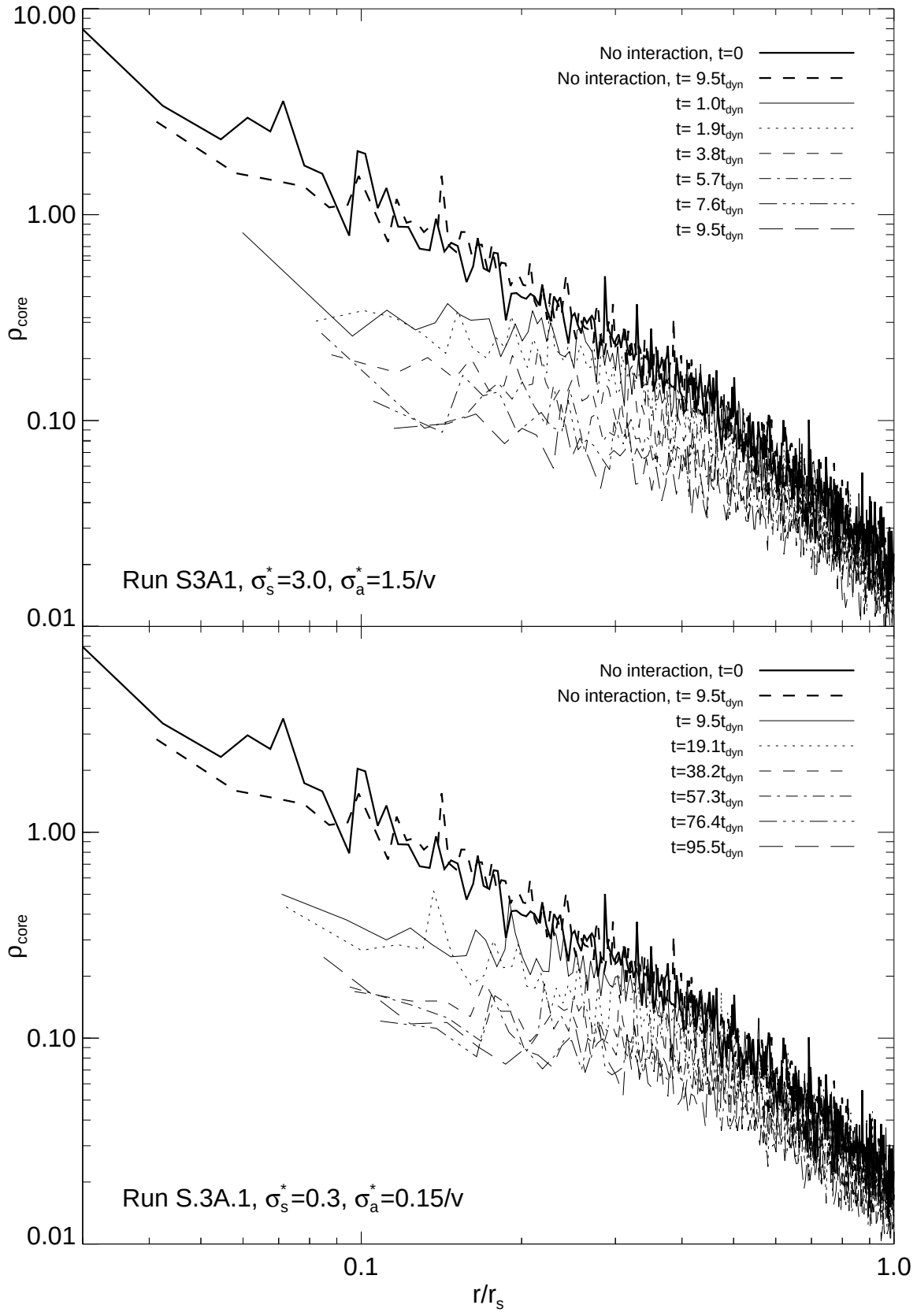

Fig. 1. Evolution of density profile in two models with annihilation and scattering. The heavy lines in both plots show the change in core behavior without interactions. In the top plot, the force softening length is 0 .01; in the bottom plot it is 0.05. In this and later density plots, only the central region of the halo is shown; the density profile does not change significantly over the course of the simulations for

a persistent core in simulations of *isolated* halos. It is unclear whether or not cores persist in high resolution simulations of halo formation in a cosmological setting (Yoshida et al., 2000; Davé et al., 2001).

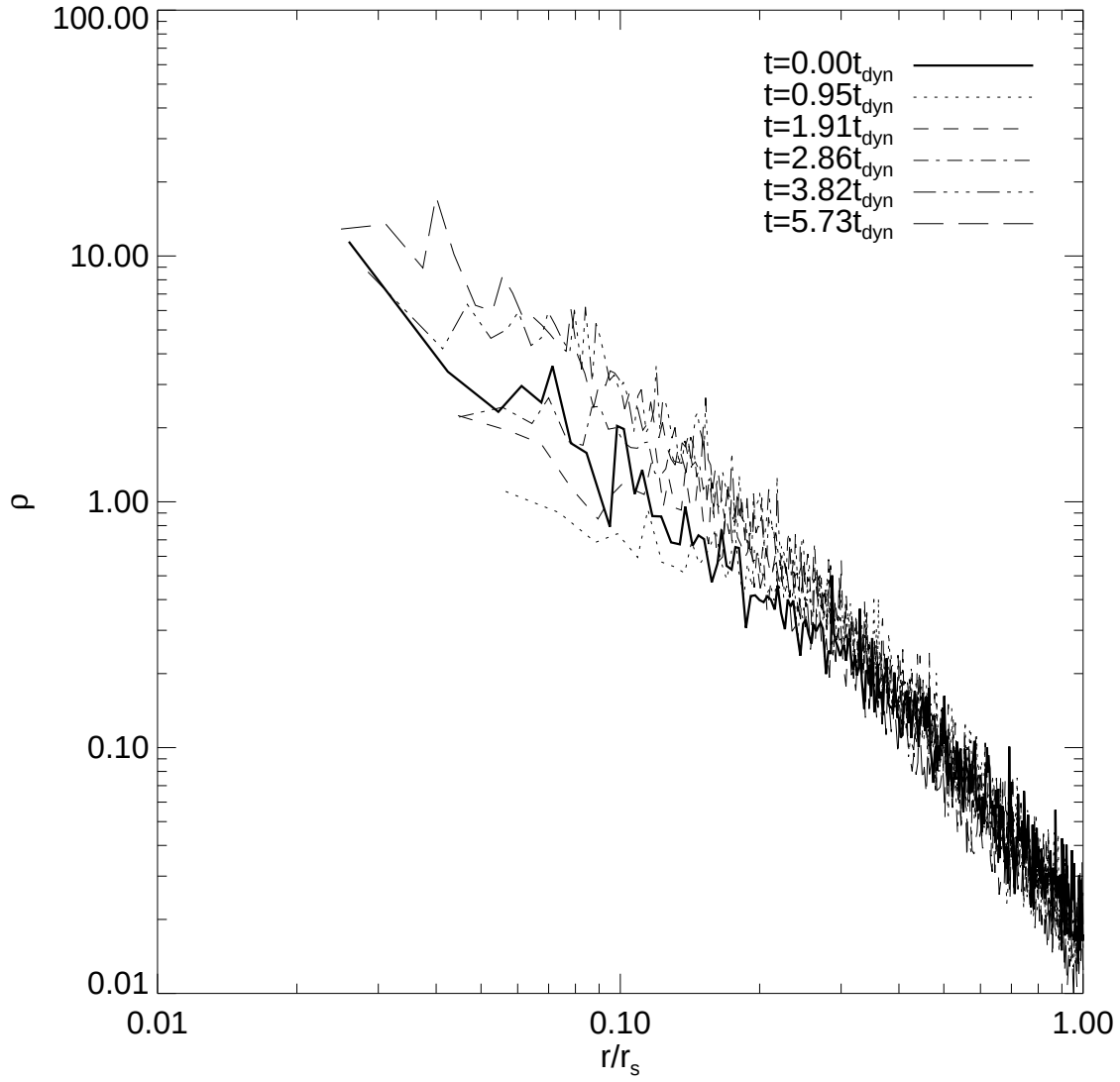

Fig. 2. Evolution of density profile in the scattering-only model S3A0. The core density initially decreases, but then begins to grow with time.

In order to differentiate between direct mass loss from annihilation and a change in the density profile due to a change in gravitational potential, we calculate the change in number density of simulation particles as a function of radius. If direct mass loss due to annihilation is causing most of the decline seen in the density profile, the number density profile ought to be unchanged,

density became so large that the typical particle was moving more than one mean free path in a time step.

with particles in the central region of the halo simply becoming less massive. Instead, as can be seen in Figure 3, which shows the evolution in the number density of particles early in the simulation, we find that the number density rapidly diminishes in the center of the halo, indicating that much of the change in central density is due to the motion of particles away from the center, not from direct mass loss. The trend of particle number density decreasing in the center continues throughout the simulation, as can be seen from Figure 1. Density profiles are calculated with a fixed number of particles per bin, so the location of the first point in the density profile is a radius that encloses a fixed number of particles; this point moves farther from the origin throughout the simulation. Furthermore, the total mass lost by the halo over the entire simulation is only 12% of the initial halo mass.

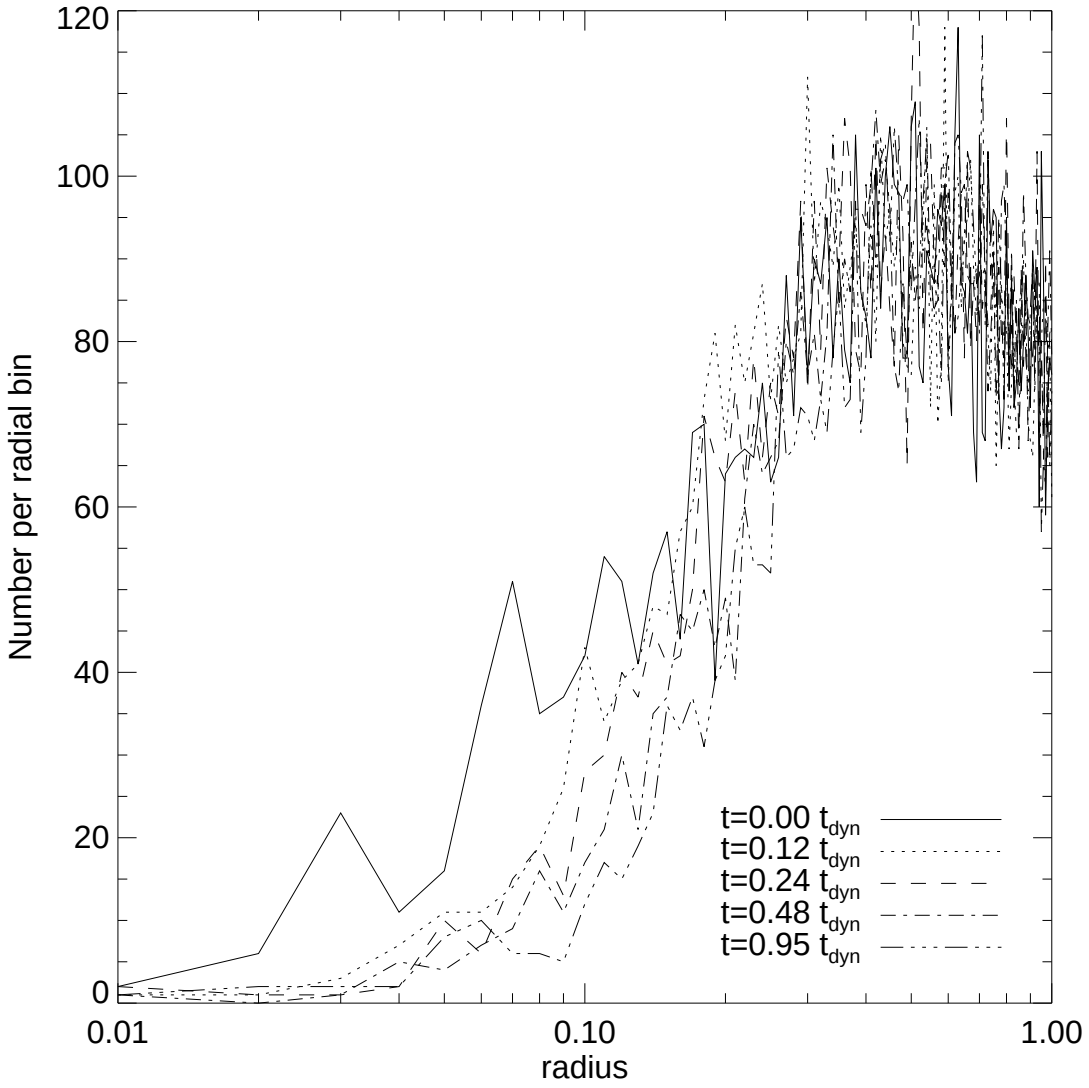

Fig. 3. Evolution in number density of particles in annihilation+scattering model.

The halo in the annihilating model forms a core very rapidly, and the size of the core continues to grow over the course of the simulation. We fit two different functional forms to the density profile of the halo. One is a modification of the initial Hernquist profile 1 to allow for a core,

$$\rho_C = \frac{\rho_0 x_c}{(x + x_c)(1 + x)^3}, \tag{10}$$

where $x = r/r_s$, and $x_c = r_c/r_s$ is the core radius in units of the scale radius. The other density profile was derived by Kaplinghat et al. (2000); their profile takes into account modifications of the initial halo density profile due to direct annihilation only, without scattering. Adiabatic expansion of the core as mass is lost decreases the core density. We have derived the profile appropriate for an initial Hernquist model,

$$\rho = \frac{\rho_0 x_c}{x(1 + x)^3 + x_c} \tag{11}$$

(note that x_c is related to the annihilation cross section in Kaplinghat's model (Eq. 13); in doing our fits we have treated x_c as a free parameter to see how well the shape of the density profile is fit by the function). Fits to both functions are shown at four different epochs in Figure 4. The two profiles differ only in the innermost region of the halo. Burkert (1995) found that dwarf galaxies are well fit by the profile

$$\rho_B = \frac{\rho_0 r_c^3}{(r + r_c)(r^2 + r_c^2)}, \tag{12}$$

where ρ_0 is the central density of the halo, and r_c its core radius. We do not expect the Burkert profile to be a good fit to our halo because the initial halo profile has both a different radial dependence at large radii, and a length scale (the scale radius) in the initial conditions separate from the core radius.

The halo shows a clear evolution from a Kaplinghat profile to a modified Hernquist profile. At early times, the Kaplinghat model is a better fit than the modified Hernquist model. At later times, the modified Hernquist model is a better fit. This is good news, because the modified Hernquist profile is closer in form to the Burkert profile. The evolution in profile shape makes sense; early in the simulation the adiabatic effect of annihilation on the gravitational potential will be small, and the Kaplinghat profile should be a good fit. The core radius in the modified Hernquist profile continues to grow throughout the simulation, as shown in Figure 5. The final core radius is 3 kpc, in the range suggested by Burkert (1995) for a halo of the mass we studied.

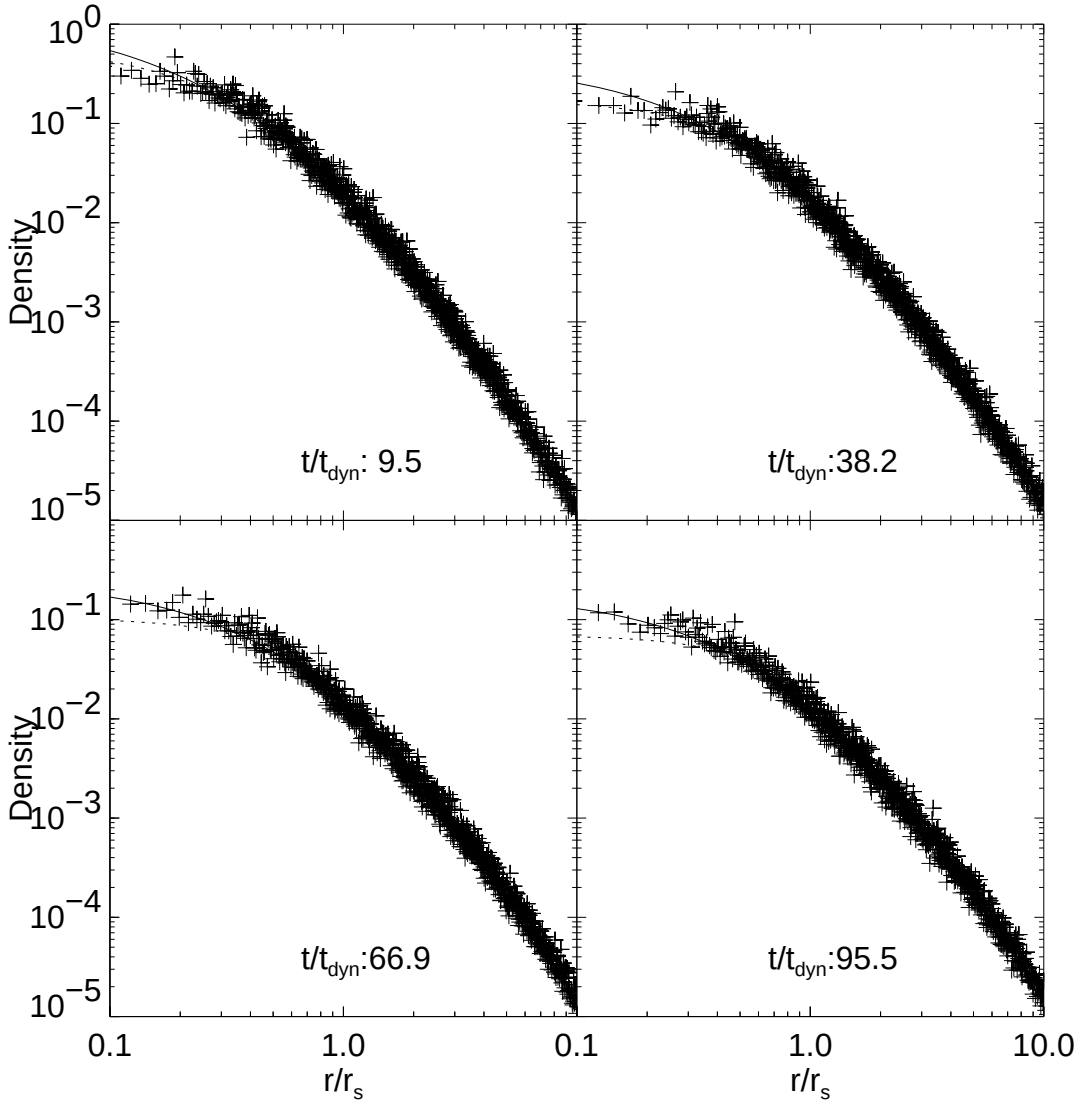

Fig. 4. Fits to the density profile of the annihilating dark matter run S.3A.1. The solid line shows the best fitting modified Hernquist profile, the dotted line the best-fitting Kaplinghat profile, and the data are the symbols. As the simulation proceeds, the halo is better fit by a modified Hernquist profile than a Kaplinghat profile.

4 Discussion

Our simulations demonstrate that annihilation produce cores of radius a few kiloparsecs in dark matter halos of dwarf galaxies; we now discuss whether this dark matter model preserves the successes of non-interacting CDM, the extent to which it addresses the problem of too much substructure in galactic dark matter halos, and the plausibility of the particle physics of the model.

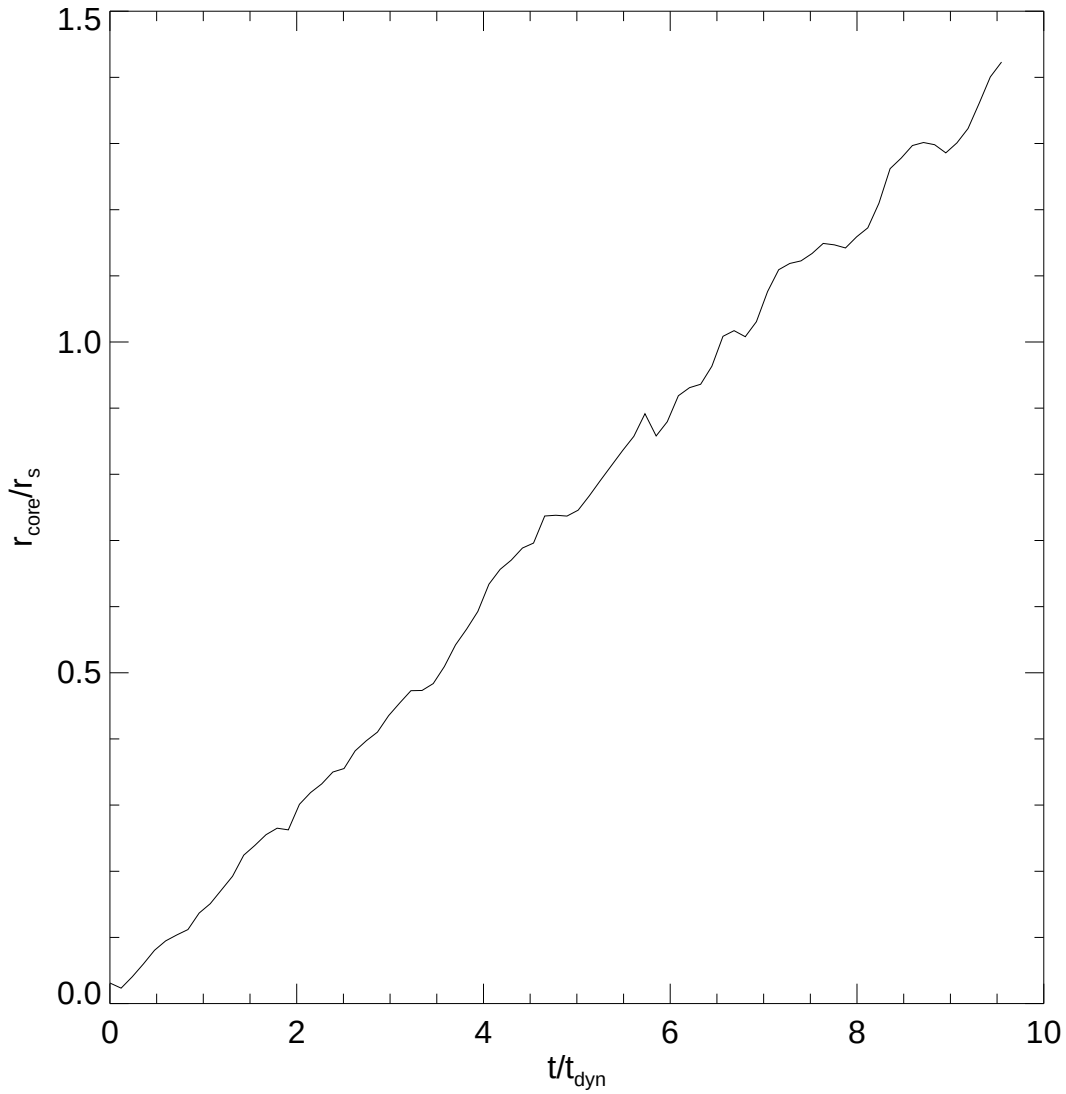

Fig. 5. Growth of the core radius with time in the annihilating DM model

There is little evidence for cores in clusters; for an annihilation model to be plausible it must modify small scale behavior of dark matter while leaving large scale behavior unchanged. In the analytic model of Kaplinghat et al. (2000), the core radius grows linearly in time, and is given by

$$x_c = \frac{r_c}{r_s} = \rho_s \sigma_a t/m = \rho_s F \sigma_a^* t \tag{13}$$

where ρ_s is the characteristic density of the NFW profile and t is the age of the halo. Since lower mass halos have higher density, and formed earlier, than high mass halos, one would expect a decreasing core radius with increasing mass. Figure 6 shows the trend of core radius with mass, assuming the core radius is given by equation (13); the core radius has been normalized to that of a

$10^{10}h^{-1}M_{\odot}$ halo (approximately 3 kpc) to eliminate the dependence of the core radius on cross section. Characteristic densities and halo ages were calculated using the Eke et al. (2000) model, assuming a $\Omega_0 = .3$, $\Omega_\Lambda = 1 - \Omega_0 = .7$ flat cosmology with $h = .65$. Most of the decrease in core radius is due to the decrease in characteristic density as mass increases; the age difference of the lowest and highest mass halo accounts for only 20% of the difference in core radius. Our model clearly creates large cores in low mass/high density halos without producing them in high mass/low density halos. Thus if the annihilations lead to a core radius of 3 kpc for dwarf galaxies, as appropriate, the predicted dark matter core radius in rich clusters would be $\sim$ 120 pc, which is deep within the central galaxy.

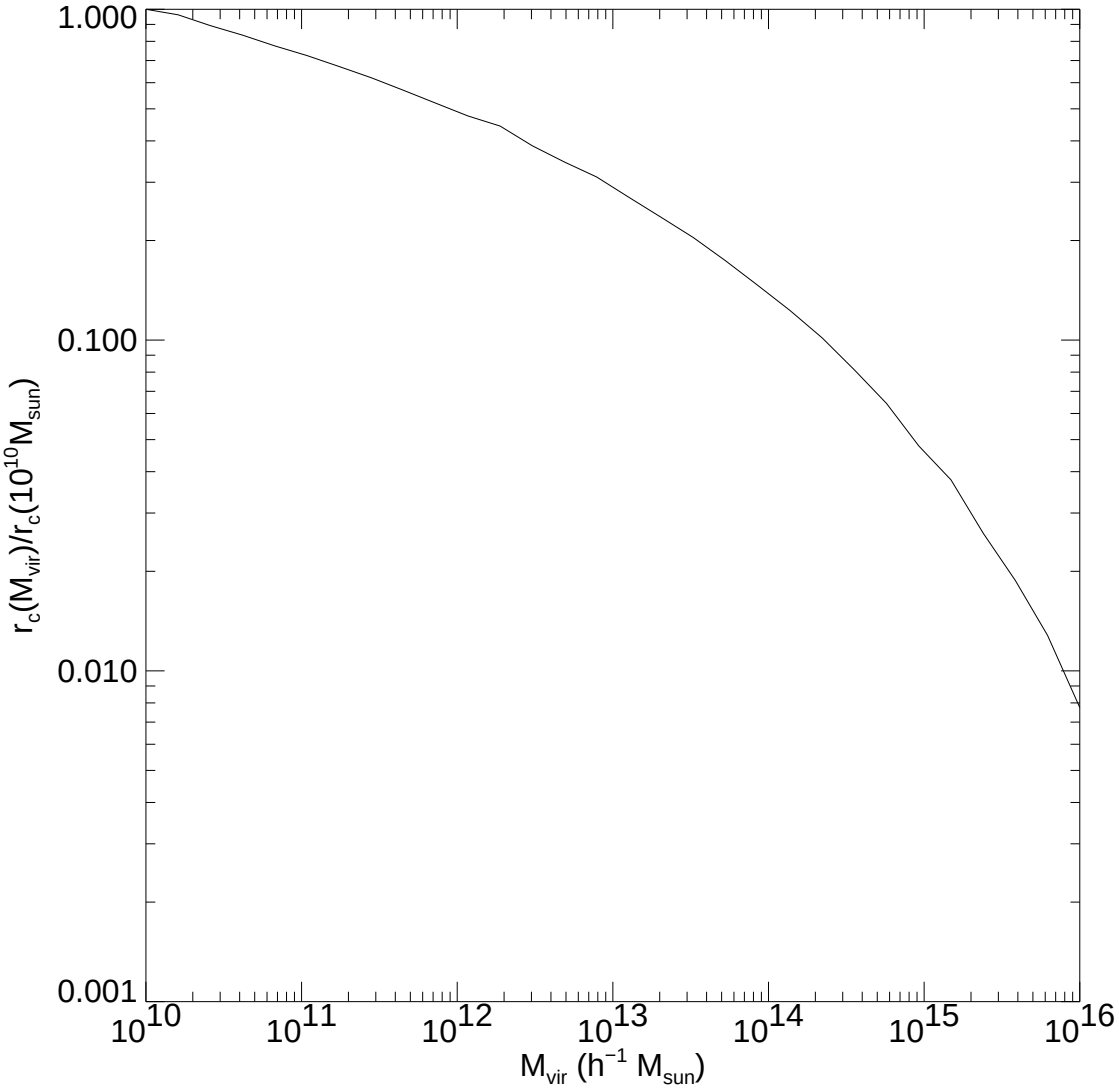

Fig. 6. Relative size of cores radius in halos of different mass.

The core structure of the dark matter halo of a high surface brightness galaxies

is unclear. Eke et al. (2000) argue that the concentrations of dark matter halos predicted in the standard ΛCDM model are consistent with both the Tully-Fisher relationship and the amount of dark matter interior to the solar radius. On the other hand, Weiner et al. (2001a) argues that detailed mass modeling of the barred spiral NGC 4123 requires either a modest core in the dark matter halo, with a core radius of 1–6 kpc, or an NFW profile with very low concentration. Arguing more generally, Debattista & Sellwood (2000, 1998) find that a high density dark matter halo in a barred galaxy leads to rapid slowing of bar rotation. For the same choice of annihilation cross-section that generates a 3 kpc core in dwarf galaxies, the core radius in a 10^{12} $M_\odot$ galaxy such as the Milky Way would be ~ 1.2 kpc, and would resolve the difficulties of bar spirals in standard ΛCDM discussed by Debattista & Sellwood (2000).

The standard ΛCDM model also predicts more substructure on galactic scales than is observed (Moore et al., 1999; Klypin et al., 1999). Although the simulations we have done cannot directly address the question of substructure, Figure 6 can be extended to low mass halos. As halo mass shrinks, the core radius increases while the virial radius increases. The two are equal for halos of mass $3\times10^7 M_\odot$; halos with mass 10^8 solar masses have a core radius that is half the virial radius. This suggests that halos smaller than a few times 10^8 solar masses would not be present in an annihilating dark matter model. Further simulation of structure formation in a cosmological context with annihilating dark matter would be helpful.

One of the problems with earlier self-interacting dark matter proposals (Carlson et al., 1992; Machacek, 1994) is that ram pressure stripping will destroy small halos too efficiently (De Laix et al., 1995). Newer models in which the dark matter behaves like a viscosity-free fluid (Peebles, 2000; Peebles & Vilenkin, 1999; Goodman, 2000; Riotto & Tkachev, 2000) avoid this problem, but may overly-suppress the growth of structure on small scales in the linear regime (Peebles, 2000), a problem shared by the earlier self-interacting dark matter models (Machacek, 1994).

The model proposed by Carlson et al. (1992) has some similarities to our model. They investigated the properties of dark matter that self-annihilated (that is, interactions occurred in which the annihilation products were the dark matter particles). Their model affects the structure of halos by heating dense regions, and affects fluctuations in the early universe through the introduction of a non-trivial Jean's length for the dark matter. Our model differs in that we assume the dark matter annihilates to something relativistic that no longer contributes to the gravitational potential of a halo after annihilation. This should lead to a greater effect on the core properties of the halo, through adiabatic changes to the gravitational potential, than the model of Carlson et al. (1992). The interacting dark matter model proposed by Spergel & Steinhardt (2000) is constructed so as to avoid excessive suppression of the power

spectrum on small scales. The dark matter is presumed to be cold, and the interaction cross sections are small enough that the probability of interaction is small at the time of recombination.

There are additional problems with an annihilating dark matter model. First, the amount of energy released in dark matter annihilation is tremendous; in our simulation of a single halo, the mass loss from annihilation (in whatever the decay products are) has an energy equivalent of 4.7×10^{45} erg s^{-1} averaged over the lifetime of the universe. This is far too large to be consistent with observations of the gamma ray background. If the dark matter annihilates, the decay products cannot include photons. Second, as discussed at length by Kaplinghat et al. (2000), the particle physics underlying an annihilating dark matter model must be carefully contrived so as to avoid complete annihilation of the dark matter in the early universe. The suppression of annihilation must be in place for $z \geq 10000$, which is a rather low energy for any reasonable phase transitions in the dark matter sector.

5 Conclusion

Annihilating dark matter leads to halo density profiles consistent with those observed in dwarf spiral galaxies. Annihilation leads to a rapid reduction in the central density of a dark matter halo, driven mainly by adiabatic expansion of the core region as matter is lost. An annihilation cross section sufficient to generate a core in a dwarf galaxy halo generates a moderate core in a Milky Way sized halo, and a negligible core in a rich cluster.

The core radius decreases rapidly with halo mass, primarily because larger objects form later in hierarchical clustering models, when the mean density of the universe is lower. Objects smaller than $\sim 3 \times 10^8 \mathrm{M}_\odot$ are unlikely to be present in an annihilating dark matter model, because the core radius will be large compared to the virial radius. A reduction in structure on this scale would be useful; CDM predicts many more halos of this size than are observed.

On the other hand, there is no compelling motivation for such a complex dark matter candidate. A special mechanism is needed to suppress annihilation of the dark matter in the early universe, and the dark matter must decay to particles that do not interact with ordinary matter. Although a particle physics model with the required properties could no doubt be constructed, such a model would be contrived.

Further study of the impact of annihilation in a cosmological setting would be useful in evaluating the promise of this model.

6 Acknowledgements

This work was supported in part by NSF grant AST00-71048.

References

Borriello, A. & Salucci, P. 2001, MNRAS, 323, 285
Burkert, A. 1995, ApJ, 447, L25
—. 2000, ApJ, 534, L143
Carlson, E. D., Machacek, M. E., & Hall, L. J. 1992, ApJ, 398, 43
Davé, R., Spergel, D. N., Steinhardt, P. J., & Wandelt, B. D. 2001, ApJ, 547, 574
De Laix, A. A., Scherrer, R. J., & Schaefer, R. K. 1995, ApJ, 452, 495
Debattista, V. P. & Sellwood, J. A. 1998, ApJ, 493, L5
—. 2000, ApJ, 543, 704
Eke, V. R., Navarro, J. F., & Steinmetz, M. 2000, astro-ph/0012337
Flores, R. A. & Primack, J. R. 1994, ApJ, 427, L1
Ghigna, S., Moore, B., Governato, F., Lake, G., Quinn, T., & Stadel, J. 2000, ApJ, 544, 616
Goodman, J. 2000, New Astronomy, 5, 103
Hernquist, L. 1990, ApJ, 356, 359
Hu, W., Barkana, R., & Gruzinov, A. 2000, Phys. Rev. Lett., 85, 1158
Hui, L. 2001, Phys. Rev. Lett., 86, 3467
Jing, Y. P. & Suto, Y. 2000, ApJ, 529, L69
Kaplinghat, M., Knox, L., & Turner, M. S. 2000, Phys. Rev. Lett., 85, 3335
Klypin, A., Kravtsov, A. V., Valenzuela, O., & Prada, F. 1999, ApJ, 522, 82
Klypin, A. A., Kravtsov, A. V., Bullock, J. S., & Primack, J. R. 2000, ApJ, accepted, astro-ph/0006343
Kochanek, C. S. & White, M. 2000, ApJ, 543, 514
Kusenko, A. & Steinhardt, P. J. 2001, astro-ph/0106008
Mac Low, M. 2001, in American Astronomical Society Meeting, Vol. 198, 5204
Machacek, M. E. 1994, ApJ, 431, 41
Moore, B. 1994, Nature, 370, 629
Moore, B. 2001, to appear in Proceedings of the 20th Texas Symposium on Relativistic Astrophysics, astro-ph/0103100
Moore, B., Ghigna, S., Governato, F., Lake, G., Quinn, T., Stadel, J., & Tozzi, P. 1999, ApJ, 524, L19
Navarro, J. F., Eke, V. R., & Frenk, C. S. 1996a, MNRAS, 283, L72
Navarro, J. F., Frenk, C. S., & White, S. D. M. 1996b, ApJ, 462, 563
Okumura, S. K., Makino, J., Ebisuzaki, T., Fukushige, T., Ito, T., Sugimoto, D., Hashimoto, E., Tomida, K., & Miyakawa, N. 1993, PASJ, 45, 329
Peebles, P. J. E. 2000, ApJ, 534, L127

Peebles, P. J. E. & Vilenkin, A. 1999, Phys. Rev. D, 60, 19452
Riotto, A. & Tkachev, I. 2000, Phys. Lett. B, 484, 177
Salucci, P. 2001, MNRAS, 320, L1
Salucci, P. & Burkert, A. 2000, ApJ, 537, L9
Sellwood, J. & Kosowsky, A. 2000, to appear in "Gas & Galaxy Evolution", astro-ph/0009074
Spergel, D. N. & Steinhardt, P. J. 2000, Phys. Rev. Lett., 84, 3760
van den Bosch, F. C. & Swaters, R. A. 2000, MNRAS, accepted, astro-ph/0006048
Wandelt, B. D., Dave, R., Farrar, G. R., McGuire, P. C., Spergel, D. N., & Steinhardt, P. J. 2000, proceedings of Dark Matter 2000, in press (astro-ph/0006344)
Weiner, B. J., Sellwood, J. A., & Williams, T. B. 2001a, ApJ, 546, 931
Weiner, B. J., Williams, T. B., van Gorkom, J. H., & Sellwood, J. A. 2001b, ApJ, 546, 916
Yoshida, N., Springel, V., White, S. D. M., & Tormen, G. 2000, ApJ, 544, L87